# An Investigation and Simulation of the Time-Dependent Behaviour of Waves in a Single-Stub Matching Network

*Alan F. Murray, Brian W. Flynn and Tim Drysdale*

## 1 Background and Aims

The primary aims of this paper are:

a) To present a new approach to teaching some extremely important, but conceptually difficult material in electromagnetism – in particular guided wave transmission.
b) An example which illustrates this approach, based on a commonly-used spreadsheet programme, along with freely-downloadable code.
c) Discussion of the way in which this simple spreadsheet-based method can be extended to explore other topics in science and engineering, with further freely-downloadable examples.

In Radio Frequency (RF) and Microwave engineering the Smith Chart [1] is used widely, as a means of visualising complex impedances and reflection coefficients. The "goodness" of an impedance match and degrees of mismatch can be seen at a glance. The Smith Chart has now been superseded by RF/microwave CAD tools for the design of transmission line systems (such as Keysight's ADS [2] and NI/AWR's Microwave Office [3]). However, these sophisticated systems still use the Smith Chart as a visualisation tool, to represent impedances graphically. Instruments such as Network Analysers also use the Smith Chart to present measured impedances graphically and it finds wide use for the depiction of the scattering parameters of both passive and active RF and microwave devices. Despite its origins over seventy-five years ago [1,4,5] as an engineer's nomograph for solving transmission line problems, the Smith Chart is still very much alive and well. It has long outlived the slide rule as an actively-used tool. It is therefore important that the Smith Chart, along with the elegant conformal mapping that it represents, is taught to and understood by students of electronic engineering, particularly those interested in analogue and RF design.

Once students have been introduced to the basics of the Smith Chart, it is often used to design matching stubs for transmission lines, to reinforce learning in a practically-important application. A matching stub is a section of transmission line, which can be either short- or open-circuited at its end, connected in parallel with a main transmission line, to cancel reflections on the line. This maximises energy transfer to the load attached to the line. Matching stubs are used in the matching of antennas with both coaxial and open wire transmission lines and, in microstrip form, for matching networks in microwave amplifiers. Unfortunately, like many design procedures, the process of matching tends to become reduced to a formulaic process in the minds of students, which masks the understanding of the operation of the stub.

The primary aim of this work is to allow students to experiment, using a simple spreadsheet-based computer simulation of a matched (and unmatched) stub. In particular, the work aims to show students "what the waves are doing" in the time domain, in parallel with a conventional Smith chart representation and a "dashboard" that acts as a matching calculator. This allows students to see the effect of changing the position and length of a stub on the incident, reflected and standing waves in the input, line and stub. The use of a spreadsheet may seem perverse, but that choice makes the simulation, which is available on http://www.teaching.eng.ed.ac.uk/open-educational-resources/electromagnetics-toy-box, usable by anyone with a Windows computer and Microsoft Excel. The calculation presented is also "checked" using an *ABCD* matrix modelling approach [6].

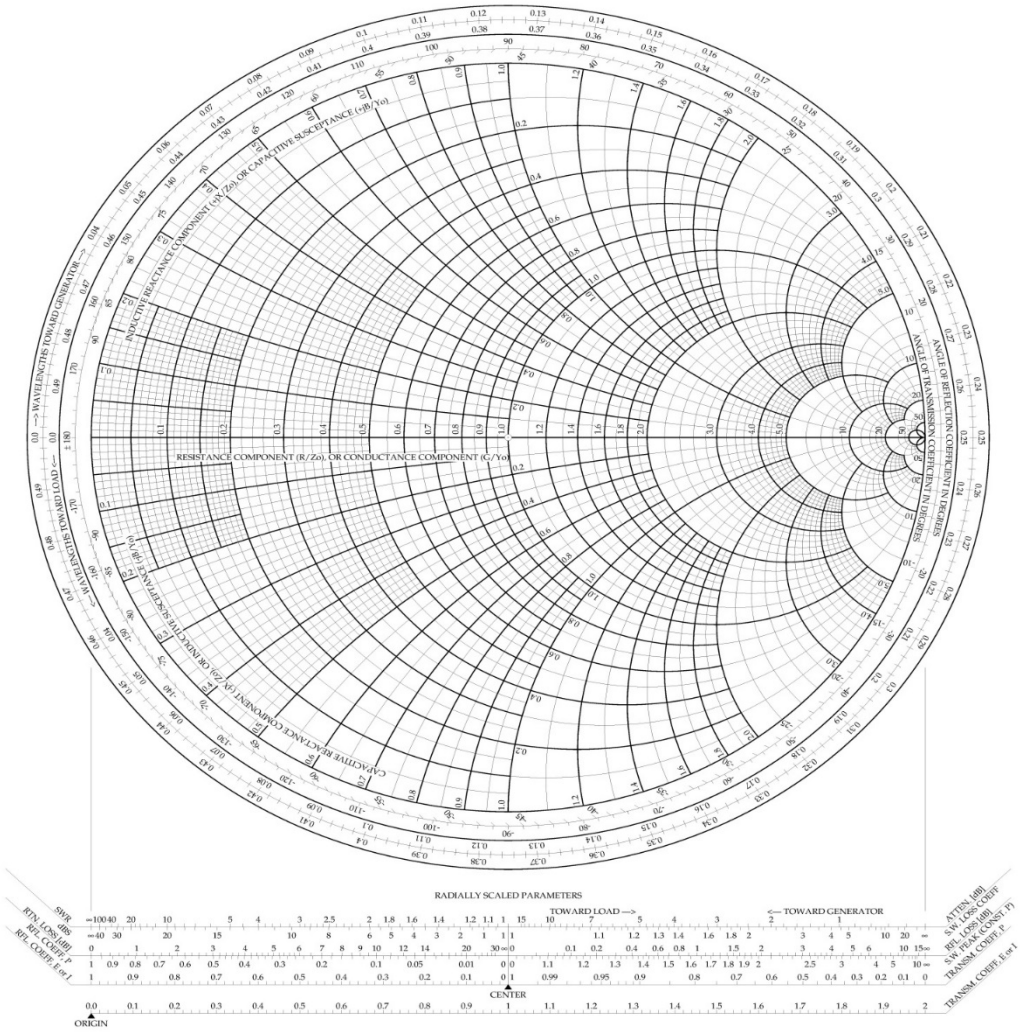


*Figure 1- The impedance Smith chart [1]*

# 2 Algebraic Analysis

## *2.1 Assumptions and Definitions*

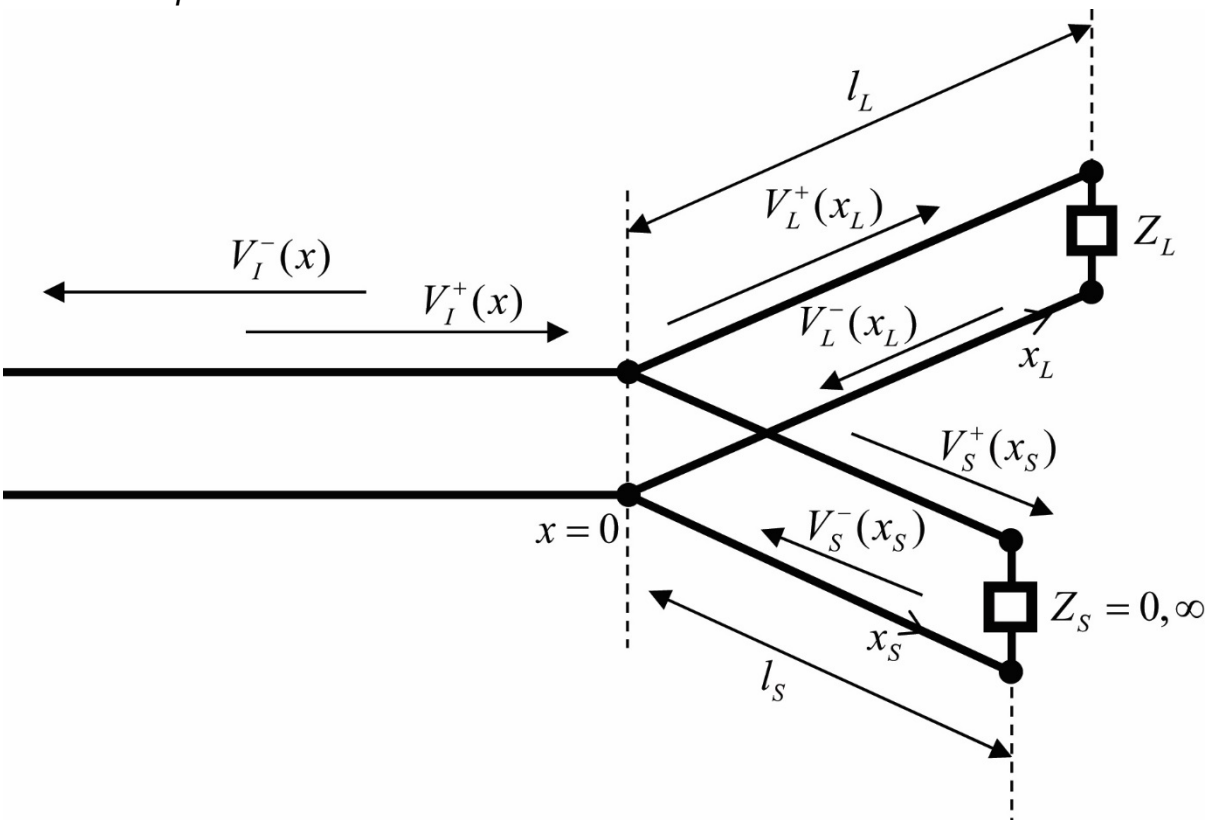


*Figure 2- Input, line and stub (schematic).* $V_L^+(x_L)$ *and* $V_S^-(x_S)$ *are the voltage of the travelling wave in the line (L) travelling left→right and right→left, respectively and all other voltages are defined in the same way. L and S are the length of the line and stub, respectively, beyond the input/line/stub junction. The load impedance is* $Z_L$ *and the stub impedance is* $Z_S$.

# 3 Notation – remove or tidy up for publication

$Z_L(Y_L)$ = **load impedance(admittance)**

$Z_S(Y_S)$ = **stub impedance(admittance)** $= 0$ *or* $\infty$

$Z_0$ = **intrinsic impedance of cable**

$\mathbf{l}_L$ = **length of line beyond the line/stub junction**

$\mathbf{l}_S$ = **length of stub beyond the line/stub junction**

$y_{L0}$ = **line impedance at** $x = 0$

$y_{S0}$ = **stub impedance at** $x = 0$

$y_{LS}$ = **impedance of line and stub in parallel at** $x = 0$

$\rho_L$ = **complex reflection coefficient of the load, at the load**

$\rho_S$ = **reflection coefficient of the stub, at the stub**

$\rho_{L0}$ = **complex reflection coefficient of the load at x=0**

$\rho_{S0}$ = **reflection coefficient of the stub at x=0**

$\rho_{LS}$ = **complex reflection coefficient of the load and stub in parallel at x=0**

Waves are multiply reflected in and between both the line and stub. The total l-r wave in (say) the line beyond the junction is therefore a superposition of an infinite number of l-r waves of frequency ω and initially unknown phase and amplitude, leading to a **<u>total</u>** l-r wave of the form:

$$V_{Ltot}^{+}\left(x_L,t\right)=\sum_{m=0}^{m=\infty}V_{Lm}^{+}e^{j(\omega t-\beta x_L+\phi_{Lm})} \tag{2.1}$$

Where $V_{Lm}^{+}$ and $\phi_{Lm}$ are the amplitude and phase, respectively, of the mth wave. There is a similar expression for $V_{Stot}^{+}\left(x_S,t\right)$. Each superposition is therefore a sum of waves with the same frequency, wavelength and direction of propagation and can therefore be written in the form:-

$$V_{Ltot}^{+}\left(x_l,t\right)=V_L^{+}e^{j\phi_L}e^{j(\omega t-\beta x_L)} \tag{2.2}$$

$$V_{Stot}^{+}\left(x_S,t\right)=V_S^{+}e^{j\phi_S}e^{j(\omega t-\beta x_S)} \tag{2.3}$$

where $V_L^{+}$ and $V_S^{+}$ are the real, unknown, amplitudes and $\phi_L$ and $\phi_S$ are the unknown phase angles of the total l-r waves in line and stub.

The total r-l wave in the line is then of the form $V_L^{-}e^{j(\omega t+\beta x_L)}=\rho_L V_L^{+}e^{j\omega t}e^{j\phi_L}e^{-j\beta l_L}e^{j\beta(x_L-l_L)}$ where $\rho_L$ is a (complex) reflection coefficient for the load and $e^{-j\beta l_L}$ represents the phase change induced as the wave travels from $x_L=0$ to $x_L=l_L$. $V_L^{-}$ is therefore complex, by dint of the multiplication of the real $V_L^{+}$ by the (known) complex number $\rho_L e^{-j\beta l_L}$. A similar analysis holds for $V_L^{-}$.

We therefore have, for the **<u>total</u>** voltages in input, line and stub ( $V_I, V_L \; and \; V_S$ respectively) :-

$$V_I=V_I^{+}e^{j(\omega t+\beta x)}+V_I^{-}e^{j(\omega t-\beta x)} \quad \left[x<0\right] \tag{2.4}$$

$$V_L=V_L^{+}e^{j\phi_L}e^{j(\omega t-\beta x_L)}+V_L^{-}e^{j\phi_L}e^{j(\omega t+\beta x_L)} \quad \left[x>0\right] \tag{2.5}$$

$$V_S=V_S^{+}e^{j\phi_S}e^{j(\omega t-\beta x_S)}+V_S^{-}e^{j\phi_S}e^{j(\omega t+\beta x_S)} \quad \left[x>0\right] \tag{2.6}$$

Inserting (complex) reflection coefficients at $x=x_L=x_S=0$ and cancelling $e^{j\omega t}$

$$V_I=V_I^{+}\left(1+\rho_{LS}\right) \tag{2.7}$$

$$V_L=V_L^{+}e^{j\phi_L}\left(1+\rho_{L0}\right) \tag{2.8}$$

$$V_S=V_S^{+}e^{j\phi_S}\left(1+\rho_{S0}\right) \tag{2.9}$$

Where all voltages $\left\{V_I,V_L,V_S\right\}$ are **<u>now at x=0.</u>** $\rho_{L0}$ and $\rho_{S0}$ are the (complex) reflection coefficient for the stub and line as seen at x=0, "looking down" the stub or line. These are of the form $\rho_{L0}=\rho_L e^{-2j\beta l_L}$, where $l_L$ is the length of the line beyond the line-stub junction and $\rho_L$ the reflection coefficient of the load itself. Both $\rho_L$ and $\rho_S$ are therefore known. $V_{S0}^{-}=V_{S0}^{+}\rho_S$ is the

complex amplitude of the r-l wave in the line and is known once $V_{S0}^{+}$ is known. Similarly, $V_{L0}^{-} = V_{L0}^{+}\rho_L$ is the complex amplitude of the r-l wave in the stub and is known once $V_{L0}^{+}$ is known

## *3.1 Boundary Conditions*

The boundary conditions are conventional. The total voltages across the stub, line and input must be the same and current is continuous at x=0. The boundary conditions are therefore, (at x=0), using (2.7)-(2.9).

### 3.1.1 Voltage Continuity: $V_I = V_L = V_S$ at $x = 0$

$$V_I = V_L \text{ and } V_I = V_S \tag{2.10}$$

So

$$V_I^{+} + V_I^{-} = V_L^{+} e^{j\phi_L}\left(1 + \rho_{L0}\right) \tag{2.11}$$

and

$$V_I^{+} + V_I^{-} = V_S^{+} e^{j\phi_S}\left(1 + \rho_{S0}\right) \tag{2.12}$$

### 3.1.2 Current Continuity: $\left(\Sigma\, currents\ in\ =\ \Sigma\, currents\ out\right)$

$$I_I^{+} + I_S^{-} + I_L^{-} = I_I^{-} + I_S^{+} + I_L^{+} \tag{2.13}$$

$$\frac{V_I^{+}}{Z_I} + \frac{V_S^{-}}{Z_S} + \frac{V_L^{-}}{Z_L} = \frac{V_I^{-}}{Z_I} + \frac{V_S^{+}}{Z_S} + \frac{V_L^{+}}{Z_L} \tag{2.14}$$

We set the characteristic impedance of all cables to be equal for simplicity, and with no loss of generality: $Z_L = Z_S = Z_I = Z_0$.

Then we have:

$$V_I^{+} + V_S^{-} + V_L^{-} = V_I^{-} + V_S^{+} + V_L^{+} \tag{2.15}$$

$$V_I^{+} + V_S^{-} e^{j\phi_S} + V_L^{-} e^{j\phi_L} = V_I^{-} + V_S^{+} e^{j\phi_S} + V_L^{+} e^{j\phi_L} \tag{2.16}$$

$$V_I^{+}\left(1 - \rho_{LS}\right) = V_S^{+} e^{j\phi_S}\left(1 - \rho_{S0}\right) + V_L^{+} e^{j\phi_L}\left(1 - \rho_{L0}\right) \tag{2.17}$$

The equations to be solved are therefore(2.11), (2.12) and (2.17), reiterated below for clarity.

$$V_I^{+}\left(1 + \rho_{LS}\right) = V_L^{+} e^{j\phi_L}\left(1 + \rho_{L0}\right) \tag{2.18}$$

$$V_I^{+}\left(1 + \rho_{LS}\right) = V_S^{+} e^{j\phi_S}\left(1 + \rho_{S0}\right) \tag{2.19}$$

$$V_I^{+}\left(1 - \rho_{LS}\right) = V_S^{+} e^{j\phi_S}\left(1 - \rho_{S0}\right) + V_L^{+} e^{j\phi_L}\left(1 - \rho_{L0}\right) \tag{2.20}$$

Solving (2.18) and (2.19) as simultaneous equations yields:-

$$V_L^{+} e^{j\phi_L} = \frac{\left(1 + \rho_{S0}\right)\left(1 - \rho_{LS}\right)}{2\left(1 - \rho_{L0}\rho_{S0}\right)} V_I^{+} \tag{2.21}$$

$$V_S^+ e^{j\phi_S} = \frac{(1+\rho_{L0})(1-\rho_{LS})}{2(1-\rho_{L0}\rho_{S0})} V_I^+ \tag{2.22}$$

It can be shown that these satisfy:-

a) The voltage boundary conditions expressed in (2.18) and (2.19).
b) The current boundary(2.20).

In addition to the boundary conditions that $V_L = V_S$, we must also check that $V_I = V_S$ and $V_I = V_L$. In other words, that, using, for example,(2.21),

$$V_I^+ (1+\rho_{LS}) = \frac{(1+\rho_{S0})(1-\rho_{LS})(1+\rho_{L0})}{2(1-\rho_{L0}\rho_{S0})} \tag{2.23}$$

After some manipulation, this yields:

$$\rho_{LS} = \frac{\rho_{L0} + \rho_{S0} + 3\rho_{L0}\rho_{S0} - 1}{\rho_{L0} + \rho_{S0} - \rho_{L0}\rho_{S0} + 3} \tag{2.24}$$

The meaning of this equation is clear if we substitute for $\rho_{L0}$ and $\rho_{S0}$ in terms of $y_{L0}$ and $y_{S0}$, the normalised admittances at x=0 of the line and stub, respectively.

$$\rho_{L0} = \frac{1-y_{L0}}{1+y_{L0}}, \quad \rho_{S0} = \frac{1-y_{S0}}{1+y_{S0}} \tag{2.25}$$

Substituting these in (2.24) gives

$$\rho_{LS} = \frac{\left(\frac{1-y_{L0}}{1+y_{L0}}\right) + \left(\frac{1-y_{S0}}{1+y_{S0}}\right) + 3\left(\frac{1-y_{L0}}{1+y_{L0}}\right)\left(\frac{1-y_{S0}}{1+y_{S0}}\right) - 1}{\left(\frac{1-y_{L0}}{1+y_{L0}}\right) + \left(\frac{1-y_{S0}}{1+y_{S0}}\right) - \left(\frac{1-y_{L0}}{1+y_{L0}}\right)\left(\frac{1-y_{S0}}{1+y_{S0}}\right) + 3} \tag{2.26}$$

After some manipulation, this yields

$$\frac{1-y_{LS}}{1+y_{LS}} = \frac{1-y_{L0}-y_{S0}}{1+y_{L0}+y_{S0}} \tag{2.27}$$

This is simply the well-known result that the admittance of the line and stub together ( $y_{LS}$ ) is equal to the sum of the two parallel admittances of the line, $y_{LS} = y_{L0} + y_{S0}$, at x=0.

### *3.2 Matching Conditions, when the Admittance $y_{LS}$=1*

The matched condition is well known to be when the line and stub admittances sum to unity.

$$y_{L0} = 1 + jX,\ y_{S0} = -jX,\ \rightarrow\ y_{LS} = y_{L0} + y_{S0} = 1 \tag{2.28}$$

Such that, at matching, as expected,

$$\rho_{LS} = \frac{1-y_{LS}}{1+y_{LS}} = \frac{1-y_L-y_S}{1+y_L+y_S} = \frac{1-1-jX+jX}{1+1+jX-jX} = 0 \tag{2.29}$$

From (2.21) and (2.22)

$$V_L^+ e^{j\phi_L} = \frac{(1+\rho_{S0})(1-\rho_{LS})}{2(1-\rho_{L0}\rho_{S0})} V_I^+ \tag{2.30}$$

$$V_S^+ e^{j\phi_S} = \frac{(1+\rho_{L0})(1-\rho_{LS})}{2(1-\rho_{L0}\rho_{S0})} V_I^+ \tag{2.31}$$

And therefore,

$$V_L^- = V_L^+ e^{j\phi L} \rho_{L0} = \frac{(1+\rho_{S0})(1-\rho_{LS})}{2(1-\rho_{L0}\rho_{S0})} \rho_{L0} V_I^+ \tag{2.32}$$

$$V_S^- = V_S^+ e^{j\phi_S} \rho_{S0} = \frac{(1+\rho_{L0})(1-\rho_{LS})}{2(1-\rho_{L0}\rho_{S0})} \rho_{S0} V_I^+ \tag{2.33}$$

We can add the results from (2.32) and (2.33) to look for cancellation at x=0. Specifically, do the reflected waves, $V_{L0}^-$ and $V_{S0}^-$ add destructively at x=0 to account for the lack of a reflected wave $V_I^-$ at matching? We find that:

$$V_S^- + V_L^- = \frac{V_I^+}{2} \tag{2.34}$$

And similarly,

$$V_L^+ e^{j\phi_L} + V_S^+ e^{j\phi_S} = \frac{3}{2} V_I^+ \tag{2.35}$$

Equation *1.34* implies that the backward waves in line and stub do not simply cancel at matching and therefore that the energy in these waves is reflected into and between the line and stub, as was assumed at the beginning of this analysis. This result is slightly "disappointing" as it does not allow of an intuitively simple explanation (to students) of the matching process. In fact, the intuitively simple, and tempting, explanation based on the r-l waves in the line and stub simply cancelling one another, is wrong. Adding (2.34) and (2.35) together, however, the sum of all of the line and stub voltages at x=0 is $2 \times V_I^+$, consistent with the voltage boundary conditions in 2.2.1 above.

# 4 Simulation Tool and Results

The primary aim of the analysis in section 2.2 is to gain an insight into the dependence of the admittances, reflection coefficients and thus the travelling waves in input, line and stub. The results in section 2.2 have been used to create an Excel spreadsheet (available from http://www.teaching.eng.ed.ac.uk/open-educational-resources/electromagnetics-toy-box) to allow system parameters to be entered, along with the signal frequency.

Figure 3 shows the Excel worksheet that allows system parameters to be entered and their influence visualised on the Smith chart, phasor diagram and line and stub admittances at x=0.

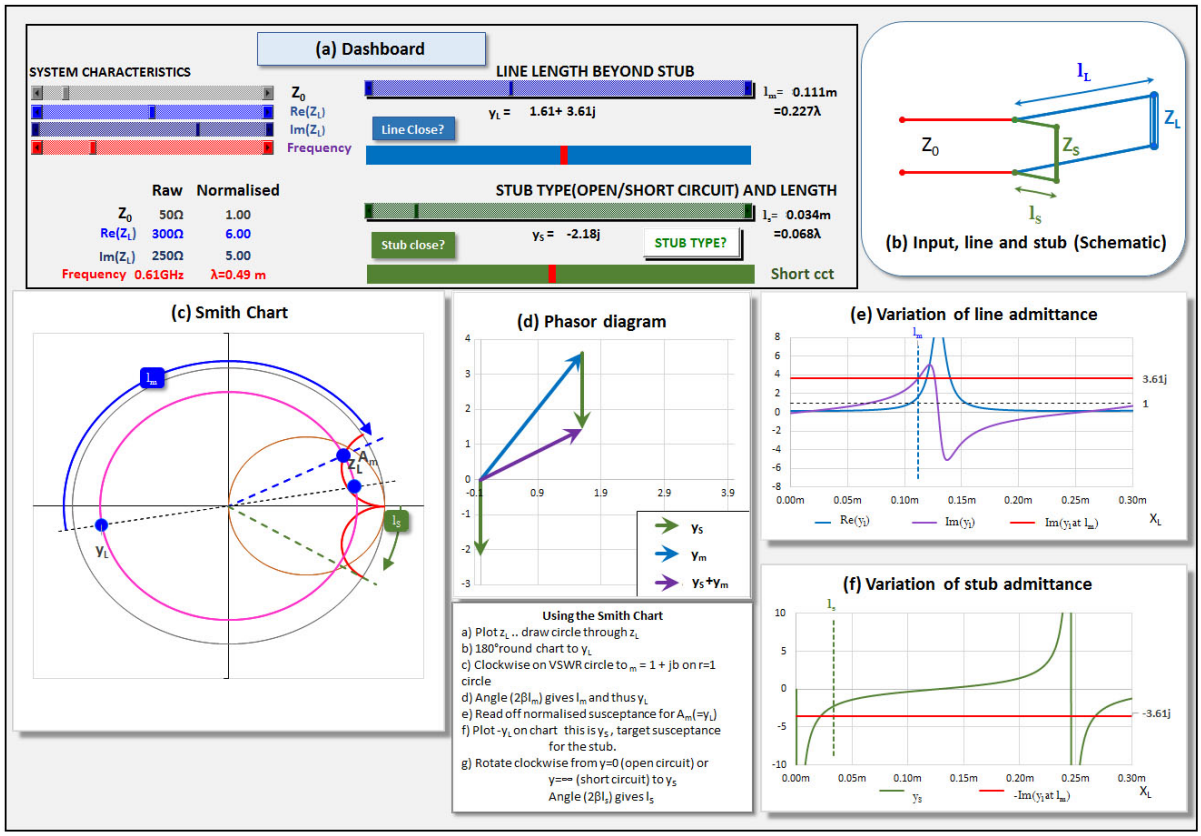


*Figure 3 - Screenshot of the input screen of the Excel simulation tool. The cable impedance is 50Ω, the load is 15+20jΩ and the stub is not matched:*
*a) The "dashboard" for entering system parameters*
*b) Schematic of the input, line and stub as presented in Figure 2 and Figure 3.*
*c) Smith chart*
*d) Phasor diagram*
*e) The variation in x of the admittance of the line, beyond the input→line+stub junction*
*f) The variation in x of the admittance of the stub, beyond the input→line+stub junction*

We will take each of these detailed components in order.

## *4.1 Dashboard*

The system dashboard allows the user to select

- the characteristic impedance of the line
  - common to input, line and stub in this example
- the signal frequency
- the (complex) load impedance
- the stub type (open circuit or short circuit)

- The length of the line beyond the line/stub junction (L in Figure 2)
- The length of the stub beyond the line/stub junction (S in Figure 2)

Figure 4 and Figure 5 show the dashboard for a line and stub under matched and unmatched conditions respectively. All parameters are set by "slider" controls and the effect of matching is highlighted clearly in Figure 5.

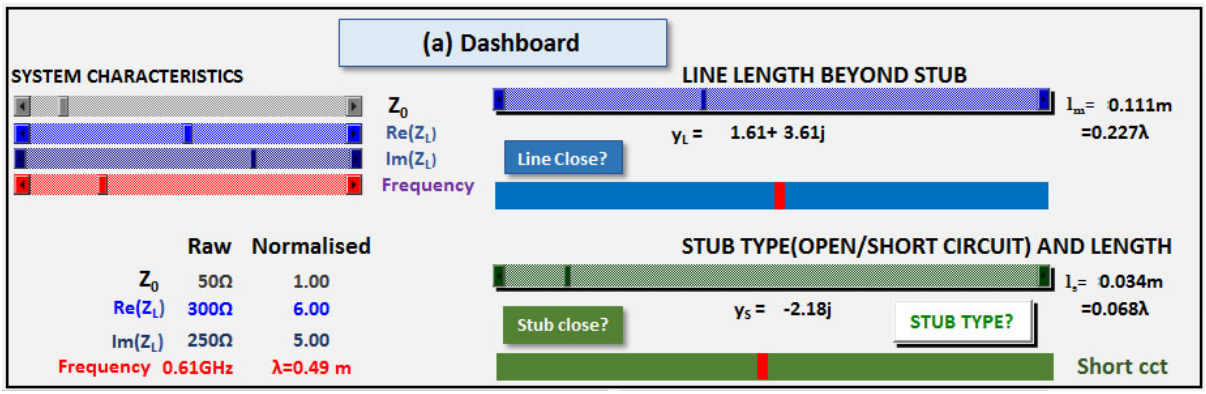


*Figure 4 - System Dashboard for an **unmatched line and stub**. The cable impedance is 50Ω, the load is 15+20jΩ and the 0.266m stub is not matched.*

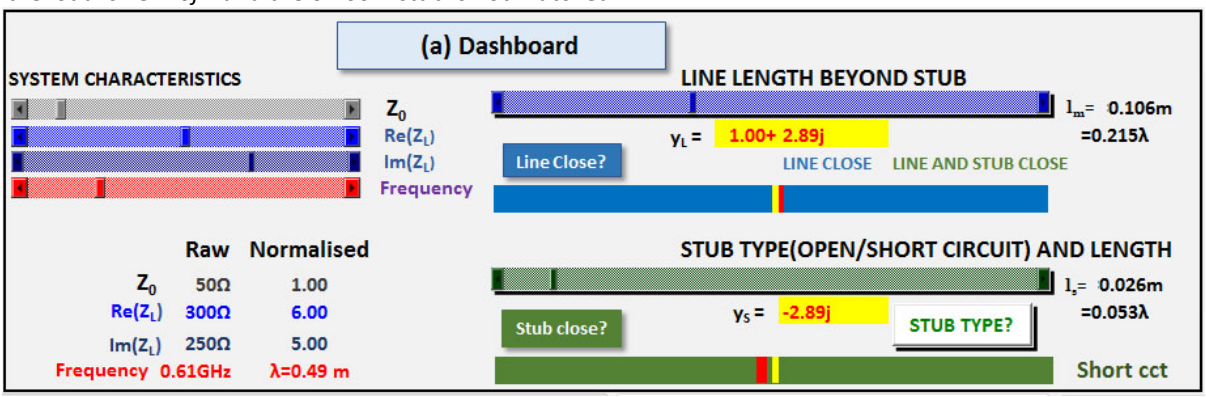


*Figure 5 - System Dashboard for a **matched line and stub**. The cable impedance is 50Ω, the load is 15+20jΩ . The line length beyond the stub is 0.216m and the (open circuit) stub length is 0.207m. Settings close to the matching condition ($A_{line}$=1+jX, $A_{stub}$=-jX) are highlighted by the yellow highlights on the stub and line admittances and by the yellow markers on the blue and green "meters" labelled "Line Close" and "Line and Stub close". The match is achieved by $A_{line}$ =1.00+1.47j and $A_{stub}$ = -1.47j.*

## 4.2 Smith Chart

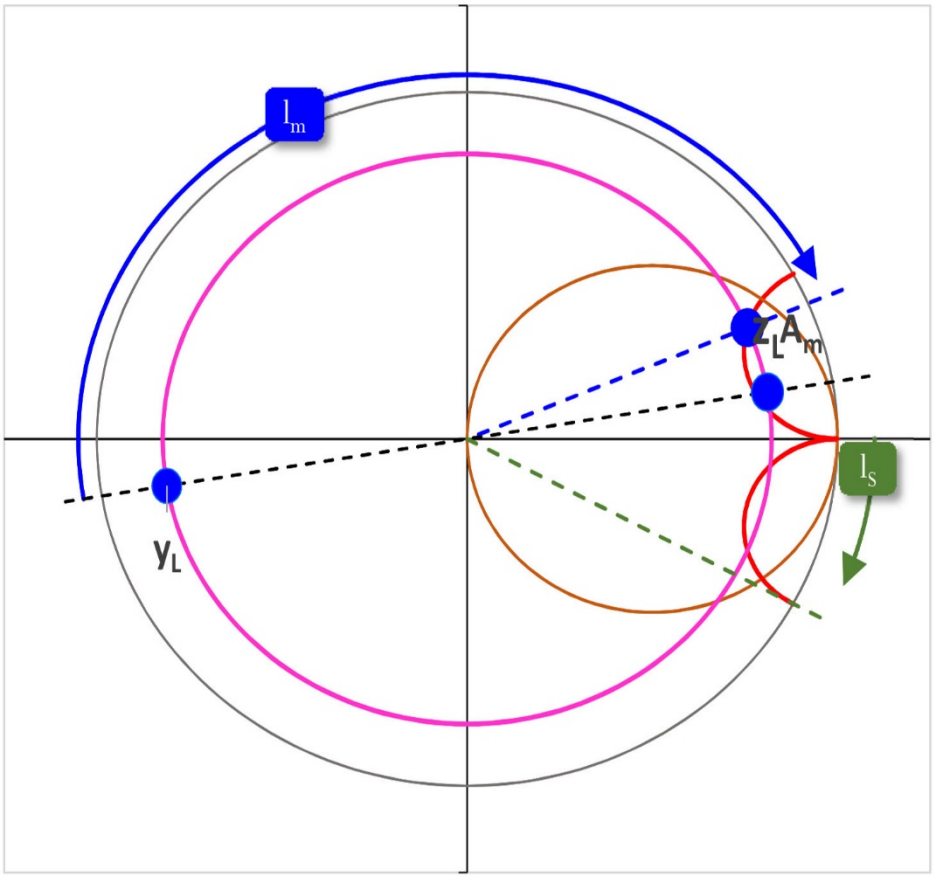


*Figure 6 - Smith chart for the matched system in Figure 5*

## 4.3 Phasor Diagram

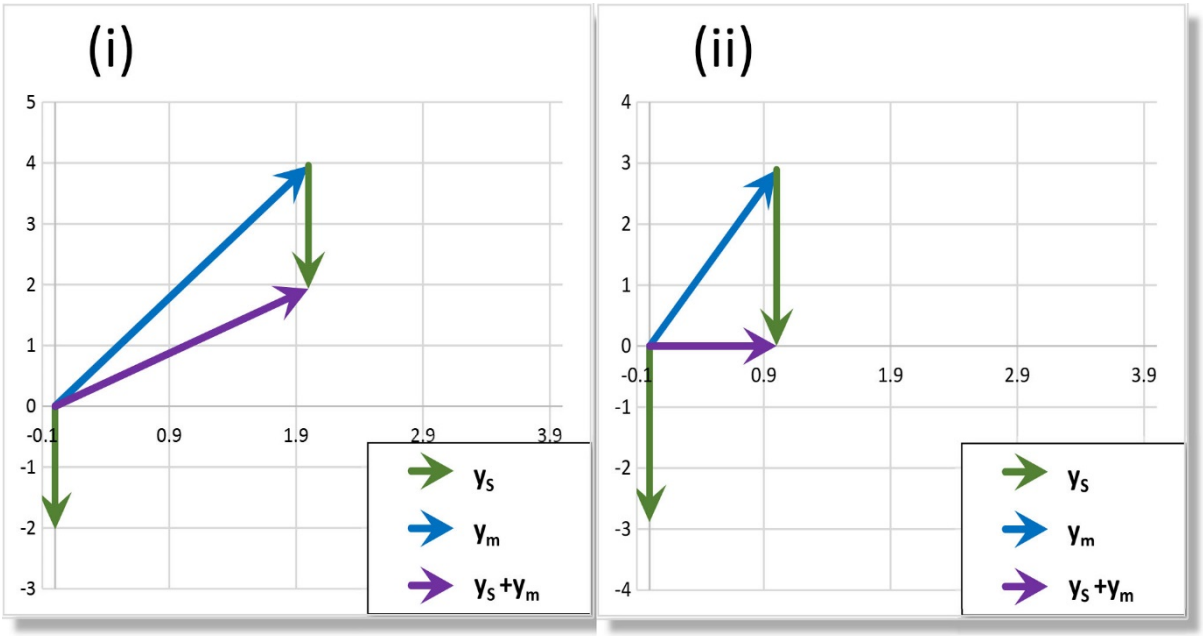


*Figure 7 - Phasor diagram for $y_{line}$, $y_{stub}$ and $y_{total} = y_{line} + y_{stub}$ in unmatched (i) and (ii) matched conditions.*

## 4.4 Line Admittance

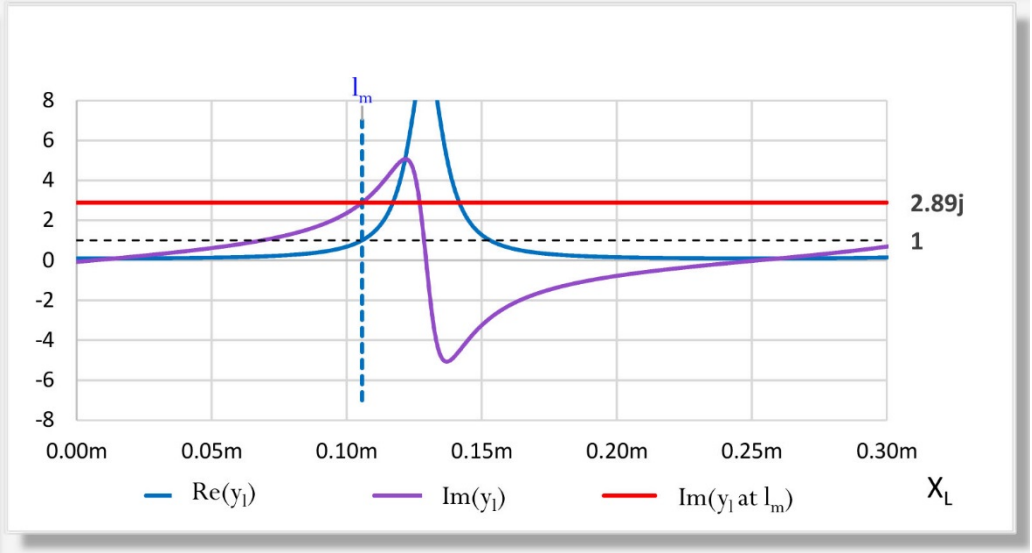


*Figure 8 - Line admittance under matching conditions. The match is achieved by $y_{line}$ =1.00+1.47j and $y_{stub}$ = -1.47j, L=0.216m. (see Figure 5).*

## 4.5 Stub Admittance

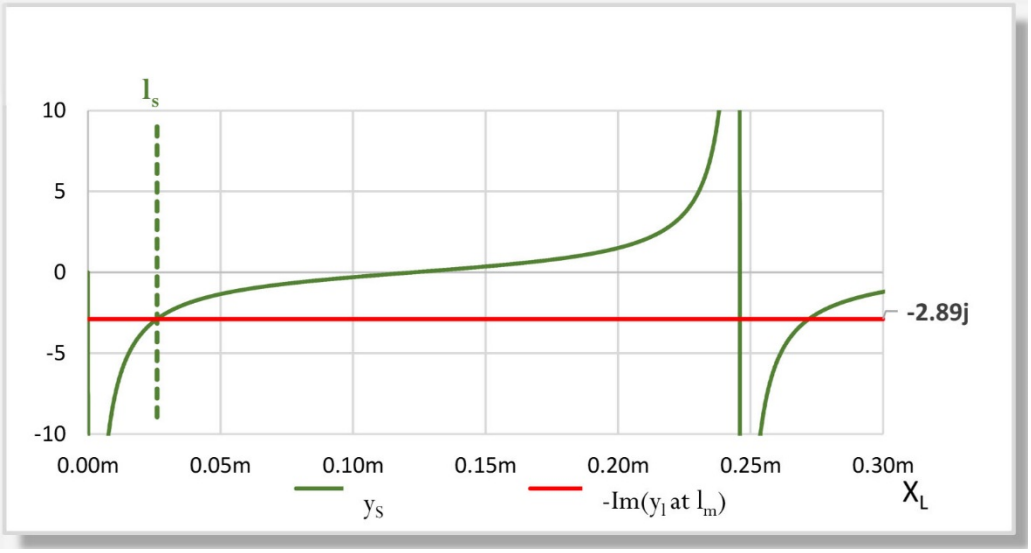


*Figure 9 - Stub admittance under matching conditions. The match is achieved by $A_{line}$ =1.00+1.47j and $A_{stub}$ = -1.47j, S=0.207m. (see Figure 5). It can be seen that $A_{stub}$ = -2.2382j at S=0.206m (see Figure 4).*

## 4.6 Travelling Waves under Matched and Unmatched Conditions.

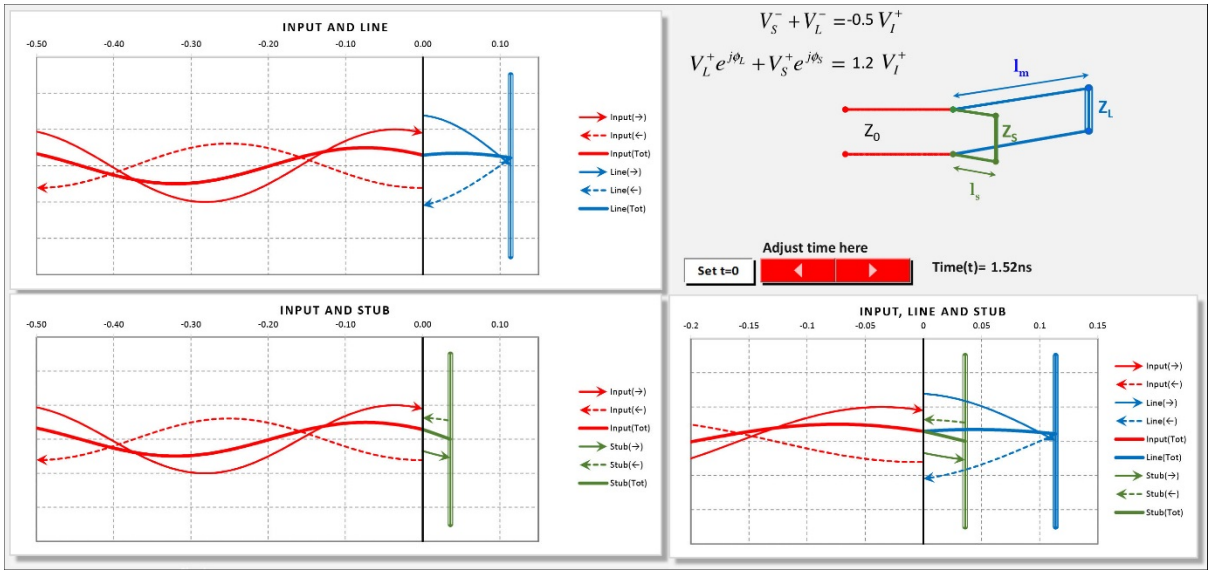


*Figure 10 - Animation of the travelling waves in input, line and stub - unmatched conditions, corresponding to Figure 4 and Figure 7(i)*

Figure 10 shows the "animation screen" that allows the travelling waves in the input, line and stub to be visualised in space and time. The red "spin button" allows time to be advanced. It can be seen that the boundary conditions in section 2.2 are satisfied, as the total voltages (incident + reflected) at x=0 in the input, line and stub are equal (heavy red, blue and green lines, respectively. This is confirmed numerically in the "Checksums" table on the bottom left.

It can also be seen that there is a reflected wave in the input line (broken red line) and that therefore the stub and line are not matched.

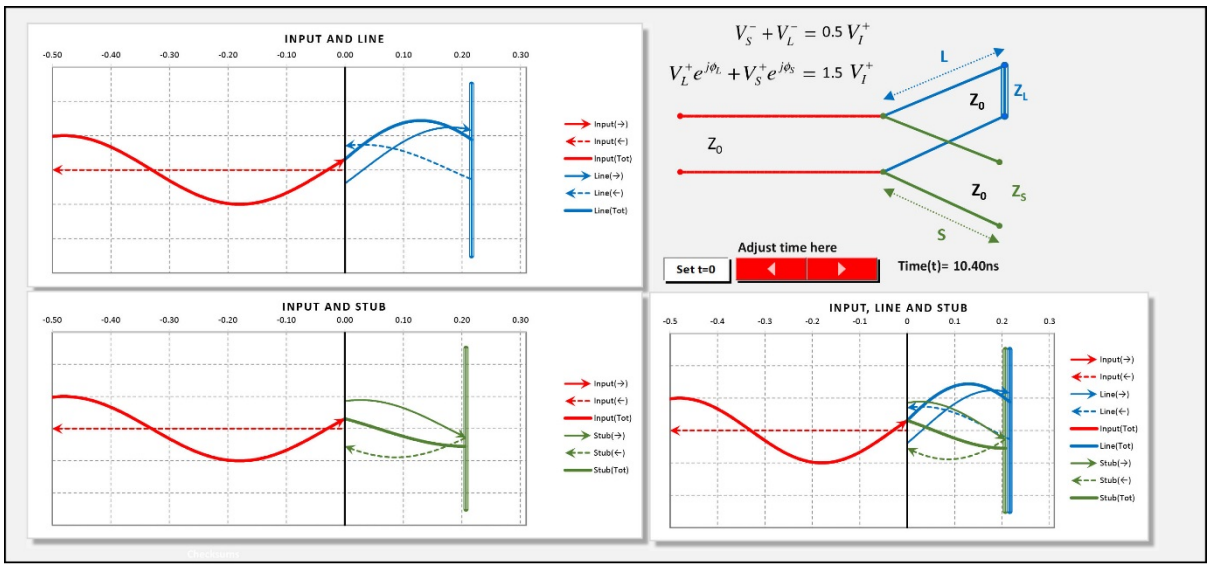


*Figure 11 - Animation of the travelling waves in input, line and stub - matched conditions, corresponding to Figure 5 and Figure 7(ii).*

Figure 11 shows the travelling waves under matched conditions. Several observations can be made:-

1) The amplitude of the reflected wave in the input (broken red line) is zero.
2) The reflected waves in the line and stub, $V_{L0}^-$ and $V_{S0}^-$, do not cancel at x=0. In fact

$V_{S0}^{-} + V_{L0}^{-} = \frac{V_I^{+}}{2}$ , confirmed by the "Checksums" table on the bottom left and consistent with the result in section 2.3.

3) The forward waves in the line and stub, $V_{L0}^{+} e^{j\phi_L}$ and , $V_{S0}^{+} e^{j\phi_S}$ sum to $\frac{3}{2} V_I^{+}$ as predicted in section 2.3 and , confirmed by the "Checksums" table on the bottom left.

These observations are clearer in Figure 12, enlarged from Figure 11. All of the results above are clearer in the simulation tool, which can be downloaded from http://www.teaching.eng.ed.ac.uk/open-educational-resources/electromagnetics-toy-box.

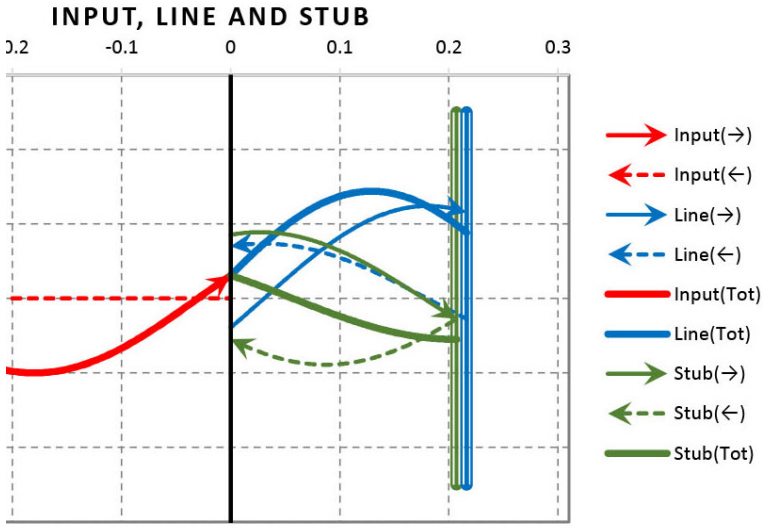


*Figure 12- All waves under matched conditions. This is enlarged from Figure 11 - Animation of the travelling waves in input, line and stub - matched conditions as shown in Figure 5 and Figure 7(ii). Note that the total voltage to the left of the stub/line junction, Input(Tot), is equal to the voltage on the right of the junction in both the line, Line(Tot) and the stub, Stub(Tot).*

## *4.7 Spreadsheet methodology – general techniques*

We have used a ubiquitous spreadsheet (Microsoft Excel) in a context for which it was not designed – dynamical simulation of a complex electronic system. Its ubiquity, however, justifies its use in this and other, teaching-related, visualisation exercises. Other examples are available in http://www.teaching.eng.ed.ac.uk/open-educational-resources/.

The key stratagems in bending Excel to this purpose are:-

1. Using time as an Excel variable.
2. Using Excel's *Activex* controls in the form of "sliders" or "scroll bars" to vary design parameters, environmental parameters (eg Figure 3) and time (eg Figure 10) , as appropriate and continuously.
    a. This latter, time, allows movement and temporal visualisation of signals and other graphical elements.
3. Using Excel's *Activex* controls in the form of toggle buttons to set binary design/environmental parameters (eg Figure 4).
4. Creative use of Excel bar graphs to produce "meters" indicating, in this case, closeness to matching conditions (eg Figure 5).
5. Creative use of Excel graphs to produce other graphical representations – in this case a

phasor diagram (Figure 7), Smith chart (Figure 6), important design parameters (eg Figure 8) and an “animated” schematic of the system (Figure 3b).

We have used this technique extensively to create a suite of simple tools that allow students to explore simple electronic circuits, complex electromagnetic phenomena and modelling processes such as finite-element analysis. Only in this latter case has Excel seen much use hitherto. Once the simple stratagems 1-5 above have been mastered, new tools can be constructed surprisingly rapidly and their identity as a simple spreadsheet concealed surprisingly effectively!

# 5 ABCD Matrix Analysis

In order to validate our analysis, we have used an ***ABCD*** matrix modelling approach. ***ABCD*** matrices relate the voltage and current on one side of a two-port network to the voltage and current on the output side [7]. They are therefore convenient for calculating the terminal properties, such as input impedance, of cascaded two-port microwave networks. Figure 13 shows the definition of voltages and currents for the ***ABCD*** matrix of a linear two port network (note that current flows *in* on the left, and *out* on the right), while the assignment of the matrix entries ***A***, ***B***, ***C***, ***D*** is as follows:

$$\begin{bmatrix} V_1 \\ I_1 \end{bmatrix} = \begin{bmatrix} \boldsymbol{A} & \boldsymbol{C} \\ \boldsymbol{B} & \boldsymbol{D} \end{bmatrix} \begin{bmatrix} V_2 \\ I_2 \end{bmatrix} \tag{4.1}$$

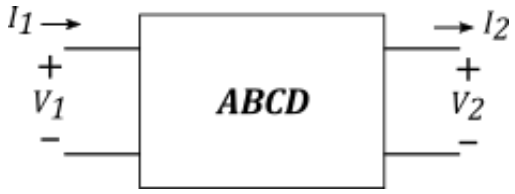


*Figure 13-Voltages and currents for the **ABCD** matrix of a two port linear network*

The educational benefits of the ***ABCD*** method have been previously reported for the case of two-wire transmission lines and baluns [8]. However, a standard transmission line equation was used in that work, to elucidate the voltages and currents at intermediate points along the transmission lines. In this section, we show:

- how intermediate voltages and currents can be directly calculated using a variant of the ***ABCD*** matrix analysis;
- the validation of the previous analysis;
- a further mathematical analysis that shows intuitively, but from a different point of view, how the ideal match extinguishes the backward wave in the section of transmission line adjacent to the generator ("the input", in section 3 above)

Our results are equally applicable to lossy transmission lines, but for clarity in the presentation we report only results for the lossless case where the ***ABCD*** matrix of a section of line is

$$\begin{bmatrix} V_1 \\ I_1 \end{bmatrix} = \begin{bmatrix} \cos(kd) & jZ_0\sin(kd) \\ \frac{j}{Z_0}\sin(kd) & \cos(kd) \end{bmatrix} \begin{bmatrix} V_2 \\ I_2 \end{bmatrix} \tag{4.2}$$

and

$$Z_0 = \sqrt{\frac{l}{c}}, \qquad k = j\omega\sqrt{lc}, \qquad \omega = 2\pi f \tag{4.3}$$

where $d$ is the length of the transmission line, $l$ and $c$ are the inductance and capacitance length, $Z_0$ is the characteristic impedance, $k$ is the propagation constant, and $f$ is the frequency. Next we recognise that any transmission line of length *d* can be equivalently represented by a single ***ABCD*** matrix or by two such matrices, one for a line of length *x* and the other for *(d-x)* where $x \leq d$:

$$\begin{bmatrix} V_1 \\ I_1 \end{bmatrix} = \begin{bmatrix} \cos(kx) & jZ_0\sin(kx) \\ \frac{j}{Z_0}\sin(kx) & \cos(kx) \end{bmatrix} \begin{bmatrix} \cos(k(d-x)) & jZ_0\sin(k(d-x)) \\ \frac{j}{Z_0}\sin(k(d-x)) & \cos(k(d-x)) \end{bmatrix} \begin{bmatrix} V_2 \\ I_2 \end{bmatrix} \quad (4.4)$$

Now if we wish to know the voltage $V_x$ and current $I_x$ at point $x$ along the transmission line, then we can simply re-arrange the equation:

$$\begin{bmatrix} V_1 \\ I_1 \end{bmatrix} \begin{bmatrix} cos(kx) & jZ_0 sin(kx) \\ \frac{j}{Z_0} sin(kx) & cos(kx) \end{bmatrix}^{-1} = \begin{bmatrix} \cos(k(d-x)) & jZ_0\sin(k(d-x)) \\ \frac{j}{Z_0}\sin(k(d-x)) & \cos(k(d-x)) \end{bmatrix} \begin{bmatrix} V_2 \\ I_2 \end{bmatrix} \quad (4.5)$$

In order for the calculation to be physically meaningful, we need to choose a source and a load. If we choose an ideal voltage source such that $V_1 = V_s$, then we need to know the characteristic impedance of the whole system to find $I_1$, which is given by

$$I_1 = \frac{V_s}{Z_{in}} \quad (4.6)$$

$Z_{in}$ can only be calculated for a given load impedance, which can be added by an ***ABCD*** matrix representing a shunt admittance with an open circuit on the right hand side, where $V_2 = V_3$, $V_2 = V_3$ and $I_3 = 0$, hence:

$$\begin{bmatrix} V_2 \\ I_2 \end{bmatrix} = \begin{bmatrix} 1 & 0 \\ \frac{1}{Z_L} & 0 \end{bmatrix} \begin{bmatrix} V_3 \\ I_3 \end{bmatrix} \quad (4.7)$$

Thus for a general two port system terminated in a load $Z_L$, the input impedance is calculated from the overall system:

$$\begin{bmatrix} V_1 \\ I_1 \end{bmatrix} = \begin{bmatrix} \boldsymbol{A} & \boldsymbol{C} \\ \boldsymbol{B} & \boldsymbol{D} \end{bmatrix} \begin{bmatrix} 1 & 0 \\ \frac{1}{Z_L} & 0 \end{bmatrix} = \begin{bmatrix} \boldsymbol{A} + \frac{\boldsymbol{B}}{Z_L} & 0 \\ \boldsymbol{C} + \frac{\boldsymbol{BD}}{Z_L} & 0 \end{bmatrix} \quad (4.8)$$

as (after rearranging to put $Z_L$ in the numerator)

$$Z_{in} = \frac{V_1}{I_1} = \frac{\boldsymbol{A}Z_L + \boldsymbol{B}}{\boldsymbol{C}Z_L + \boldsymbol{D}} \quad (4.9)$$

where ***A, B, C, D*** are the ***ABCD*** matrix entries for the overall two-port system, in this case a single stretch of transmission line as per (4.9), giving

$$Z_{in} = \frac{Z_L\cos(kd) + jZ_0\sin(kd)}{\frac{jZ_L}{Z_0}\sin(kd) + \cos(kd)} \quad (4.10)$$

Now that we know $Z_{in}$ we need to invert the matrix that we had shifted to the left hand side of (4.5). The inverse of a 2x2 matrix is

$$\begin{bmatrix} a_{11} & a_{12} \\ a_{21} & a_{22} \end{bmatrix}^{-1} = \frac{\begin{bmatrix} a_{22} & -a_{12} \\ -a_{21} & a_{11} \end{bmatrix}}{\begin{vmatrix} a_{11} & a_{12} \\ a_{21} & a_{22} \end{vmatrix}} = \frac{\begin{bmatrix} a_{22} & -a_{12} \\ -a_{21} & a_{11} \end{bmatrix}}{a_{11}a_{22} - a_{12}a_{21}} \tag{4.11}$$

Conveniently, the determinant of the matrix is unity (and using $cos^2\theta + sin^2\theta = 1$, thus

$$\begin{bmatrix} V_x \\ I_x \end{bmatrix} = \begin{bmatrix} V_1 \\ I_1 \end{bmatrix} \begin{bmatrix} \cos(kx) & jZ_0 \sin(kx) \\ \frac{j}{Z_0}\sin(kx) & \cos(kx) \end{bmatrix}^{-1} = \begin{bmatrix} V_s \\ \frac{V_s}{Z_{in}} \end{bmatrix} \begin{bmatrix} \cos(kx) & -jZ_0 \sin(kx) \\ \frac{-j}{Z_0}\sin(kx) & \cos(kx) \end{bmatrix} \tag{4.12}$$

giving

$$V_x = V_s \left( \cos(kx) - j\frac{Z_0}{Z_{in}} \sin(kx) \right) \tag{4.13}$$

$$I_x = \frac{V_s}{Z_{in}} \left( \cos(kx) - \frac{jZ_{in}}{Z_0} \sin(kx) \right) \tag{4.14}$$

Equations (4.13) and (4.14) are much more physically intuitive than the standard transmission line result:

$$Z_x = \frac{Z_2 + Z_0 \tan(\gamma(d-x))}{Z_o + Z_2 \tan(\gamma(d-x))} Z_0 \tag{4.15}$$

$$I_x = \frac{E}{Z_x \cosh(\gamma x) + Z_0 \sinh(\gamma x)} \tag{4.16}$$

and

$$V_x = Z_x I_x \tag{4.17}$$

because the Ohm's law relationship between the expressions for $V_x$ and $I_x$ in (4.13) and (4.14) is seen to fall out of the analysis rather than being forced in (compare with (4.15) and (4.16)), and the algebraic form $\cos(\theta) - j\sin(\theta)$ immediately suggests the trigonometric identity $e^{-j\theta}$, a single wave. Next, the realisation that the identity cannot be directly applied because of the factor $\frac{Z_0}{Z_{in}}$ prepending the sin function (unless $Z_0 = Z_{in}$) should suggest that under matched conditions there is only one wave (the forward wave) in the first section of the transmission line. On the other hand, when there is a mismatch and $Z_0 \neq Z_{in}$ then the magnitude of the forward and backward waves can be calculated as follows. We begin with an expression for the forward and backward waves in exponential form and convert to trigonometric form as follows

$$Me^{jkx} + Ne^{-jkx} = (M+N)\cos(kx) + j(M-N)\sin(kx) \tag{4.18}$$

From (4.13) and (4.14) we see that

$$\left(M+N\right)=1 \tag{4.19}$$

$$\left(M-N\right)=\frac{Z_{in}}{Z_0} \tag{4.20}$$

Hence

$$M=\frac{1}{2}+\frac{Z_0}{2Z_{in}} \tag{4.21}$$

$$N=\frac{1}{2}-\frac{Z_0}{2Z_{in}} \tag{4.22}$$

From this formulation, it can immediately be seen that when matched, *M =1* and *N = 0*, giving only a forward wave, whilst when unmatched, the magnitude of the backward wave increases with the degree of mismatch. This formulation emphasises the physical relevance of this mismatch upon the magnitude of the forward and backward waves. We validated this approach by using it to recalculate the data in Fig. 4 in [8].

Further, we note that the ratio of the forward to backward waves takes on the standard form of reflection coefficients, allowing the reflection coefficient to fall out of the system rather than being forced in:

$$\rho=\frac{\left|N\right|}{\left|M\right|}=\frac{\left(1-\frac{Z_0}{Z_{in}}\right)}{\left(1+\frac{Z_0}{Z_{in}}\right)}=\frac{Z_{in}-Z_0}{Z_{in}+Z_0} \tag{4.23}$$

We can apply the analysis to each section of a branched circuit, so long as the voltage and current is known on the side that has the source, and the input impedance into the rest of the circuit is known (this is the load on that section of waveguide). To illustrate this, a single stub matching circuit is considered, as shown in Figure 14.

The currents and voltages , $V_x$ and $I_x$, on the first line from the source to the junction at x = $d_{in}$, are given by (4.13) and (4.14) where $Z_{in}^{all}$ is substituted for $Z_{in}$. Note that for this analysis, we define x = 0 to be at the source.

The voltages and currents on the line to the load are $V_y$ and $I_y$, where 0 < y <$d_{load}$. Note that at y=0, x=$d_{in}$ and $V_{y=0} = V_{x=}d_{in}$. Note that when coded into a numerical calculator or mathematical programming environment, (4.13) and (4.14) can simple be reused, substituting $V_{x=din}$ , $I_{x=din}$ for $V_s$ and $I_s$. However, they can be calculated analytically by substituting those values into (4.13) and (4.14) and solving. The details are omitted for brevity, yielding

$$V_y=\frac{V_s}{4Z_{in}}\left\{\begin{array}{l} e^{jky}\left[\left(Z_{in}-1+2Z_0\right)e^{jkd_{in}}+\left(Z_{in}+1\right)e^{-jkd_{in}}\right] \\ +e^{-jky}\left[\left(Z_{in}+1\right)e^{jkd_{in}}+\left(Z_{in}-1-2Z_0\right)e^{-jkd_{in}}\right] \end{array}\right\} \tag{4.24}$$

$$I_y = \frac{V_s}{4Z_{in}} \left\{ \begin{array}{l} e^{jky}\left[\left(\frac{Z_{in}}{Z_0}-1\right)e^{jkd_{in}} + \left(3-\frac{Z_{in}}{Z_0}\right)e^{-jkd_{in}}\right] \\ +e^{-jky}\left[\left(1+\frac{Z_{in}}{Z_0}\right)e^{jkd_{in}} + \left(1+\frac{Z_{in}}{Z_0}\right)e^{-jkd_{in}}\right] \end{array} \right\} \quad (4.25)$$

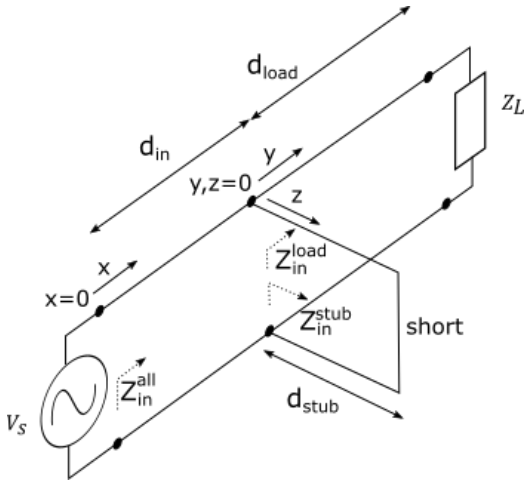


*Figure 14- Diagram and dimensions of single stub tuning circuit for transmission line with uniform characteristic impedance $Z_0$. The input impedance has been defined for three different parts of the circuit (looking into the input, looking into the line to the load.*

The currents and voltages in the stub can be found through an identical process. In order to animate the waves in time, as is done in the Excel spreadsheet with the previous analysis all that is required is to plot the real value of the voltage (or current, as desired) after re-including the time dependence that has been omitted in this section for clarity. For the sake of comparing the two techniques, we implement both sets of analyses in numerical python, omitting the graphical user interface features from the spreadsheet, and compare the absolute magnitude and phase of the forward and backward waves. Although not shown here for brevity, we also compared the python results directly with the results calculated in the spreadsheet, in order to verify the two implementations of our new analysis technique are identical. In order to do this, we needed to calculate the absolute magnitude of the voltage as a function of position on the transmission line. The Excel spreadsheet generates results at specific times, so the absolute magnitude can be obtained from data obtained a quarter-period $\left(\frac{T}{4}\right)$ later in time, by the following formula

$$|V| = \sqrt{V(0)^2 + V\left(\frac{T}{4}\right)^2} \quad (4.26)$$

We present results from the two different analysis methods for the case of the same system that we analysed earlier in paper, which had the following parameters: $Z_0$ = 50Ω, $Z_L$ = 300 +250j Ω, $f$ = 610 MHz, $d_{load}$ = 0.215λ, and $d_{stub}$ = 0.303λ, with an open circuit. The total voltages are plotted in Figure 15, and show excellent agreement. The python code for both analysis methods can be found in supplementary material here.

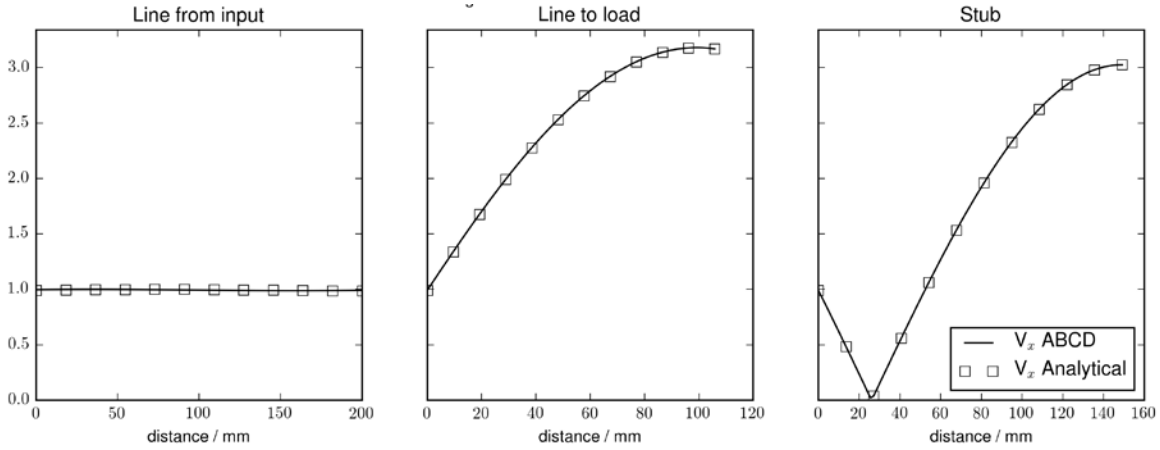


*Figure 15 – Plot of the absolute magnitude of the total voltage for an example single stub junction, comparing results from the analytical analysis and the ABCD method.*

# 6 Discussion and Conclusions

Section 2 presents a new analysis of electromagnetic waves in a stub-matched transmission line. The mathematics is straightforward, but has not, to our knowledge, been explored before. It does not of itself improve the **design** of these networks, but allows an insight into the shape and form of the waves in the input, line and stub under both matched and unmatched conditions. The design of a stub matching network involves, historically, the use of the Smith Chart. Although CAD tools now calculate the parameters of a matched network analytically, many such tools display their outputs as a Smith chart. In all cases, the time-dependence of the sinusoidal voltage and current waves in the line and stub are left unexplored. Design takes place in the impedance/reflection coefficient space, relating the two via the conformal mapping that is exemplified by the Smith chart. While this design approach is effective and elegant, it does little to help learners to visualise how the waves in the input, line and stub are "behaving" – in other words, "if we could see the waves, what would they look like?". It is clear that, in science education, understanding is underpinned and improved by effective visualisation and simulation tools [eg 9,10].

The simple Excel-based simulation tool described in section 4 allows the design parameters of simple stub-matching network to be adjusted and their influence on the design of the matched network to be visualised clearly and shown in Figure 3-Figure 9. More importantly, it allows the waves in the input line and stub to be simulated in the time domain in a familiar "oscilloscope screen" format, under both matched and unmatched conditions (Figure 10-Figure 12). Intriguingly, the simulator also proved the authors' initial preconceptions of the activity in the line and stub to be incorrect. The reflected waves from the load and stub termination do not simply cancel one another when matching is achieved. The reality is more subtle and is rooted in the (voltage continuity) boundary condition - that the total voltage on the left of the stub/line junction must be equal to the voltage on the right of the same junction in both the line and the stub (see Figure 12).

More generally, we have presented an example of a simple, spreadsheet-based "simulation" of a reasonably complex system. It is clear that a spreadsheet is not the optimal tool for complex simulation of dynamical systems. Nevertheless, spreadsheets, particularly Microsoft's Excel, are ubiquitous and generally free at the point of use to students. We therefore advocate this approach as a powerful, generic tool for enhancing learning and present a range of examples on http://www.teaching.eng.ed.ac.uk/open-educational-resources/.

# 7 References


1. Smith, P. H., *Transmission Line Calculator*, Electronics, Vol.12, p.29, January, 1939.

2 Keysight Technologies, *Advanced Design System (ADS)*, http://www.keysight.com/en/pc-1297113/advanced-design-system-ads?cc=US&lc=eng , last accessed April 2016.

3. National Instruments, *Microwave Office,* http://www.awrcorp.com/products/microwave-office , last accessed April 2016.

4. Smith, P. H., *An Improved Transmission Line Calculator*, Electronics, Vol. 17, p.130, January, 1944.

5. Pereira, J. R. Pinho, P., *Using Modern Tools to Explain the Use of the Smith Chart*, IEEE Antennas and Propagation Magazine, Vol. 52, No.2, April 2010.

6. P K Webb, British Post Office Research Department Report 630 (1977).

7. Pozar, D. M., *Microwave Engineering*, John Wiley & Sons, New York, 2nd Ed., 1998, pp. 206 - 209

8. Peres, P. L. D., de Souza C. R., Bonati, I. S., *ABCD Matrix: A Unique Tool For Linear Two-Wire Transmission Modelling*, International Journal of Electrical Engineering Education, Vol 40, No. 3, pp. 220-229, 2003

9 Perkins, K, Adams, W, Dubson, M, Finkelstein, N, Reid, S, Wieman, C and LeMaster, R, *PhET: Interactive Simulations for Teaching and Learning Physic,* Physics Teaching 44, 18 (2006)

10. Gilbert, J.K, *Visualization in Science Education*, Springer, (ISBN 978-1-4020-3613-2) 2008.